Direct Operando Spectroscopic Observation of Oxygen Vacancies in Working Ceria-Based Gas Sensors

Ann-Kathrin Elger, Julian Baranyai, Kathrin Hofmann, Christian Hess*

Eduard-Zintl-Institut für Anorganische und Physikalische Chemie, Technische Universität Darmstadt, Alarich-Weiss-Str. 8, 64287 Darmstadt, Germany

*hess@pc.chemie.tu-darmstadt.de

Keywords: oxygen vacancies, gas sensors, operando, ceria, gold, mechanisms

Abstract

Metal-oxide semiconductors are of great interest for gas-sensing applications. We provide new insights into the mode of operation of ceria-based gas sensors during ethanol gas sensing using combined *operando* Raman–gas-phase FTIR spectroscopy. Visible Raman spectroscopy is employed to monitor the presence of oxygen vacancies in ceria via F_{2g} mode softening, while simultaneously recorded FTIR spectra capture the gas-phase composition. Such an experimental approach allowing the direct observation of oxygen vacancies in metal-oxide gas sensors has not been reported in the literature. By systematically varying the gas atmosphere and temperature, we can relate the sensor response to the spectroscopic signals, enabling us to obtain new fundamental insight into the functioning of metal-oxide semiconductor gas sensors, as well as their differences to heterogeneous catalysts.

Metal-oxide semiconductors are of great interest for gas-sensing applications because of their high sensitivity to target gases and their simple fabrication.[1-3] The principle of their operation is based on the adsorption of target molecules on the semiconductor's surface inducing changes of the material's electrical conductivity. While there has been considerable progress in the field, [4-7] a detailed mechanistic understanding of the target gas-induced surface processes and their relation to the measured sensor's conductivity change is still lacking.

According to the proposed gas-sensing mechanisms, the sensor response can be explained by changes of the electric surface potential resulting from 'ionosorption' of gaseous molecules (ionosorption model) or by changes in the oxygen stoichiometry, that is, by the variation of the amount of (sub-)surface oxygen vacancies and their ionization (reduction–reoxidation mechanism). In fact, it has been proposed in the literature, that the target gas (e.g. CO) removes oxygen from the surface of the lattice yielding adsorbed species and/or gas-phase products (e.g.

CO_2) in a process, which is accompanied by the formation of an oxygen vacancy. As a result of vacancy ionization, electrons are released into the conduction band, thereby increasing the conductivity of the gas sensor. In the presence of oxygen, the vacancy is filled again by taking electrons from the conduction band, leading to a decrease in conductivity. However, as pointed out previously,[2,4] there are several open questions, such as the type of surface oxygen involved in the reaction with the target gas (e.g. O^-, O_2^-), and the role of oxygen diffusion into the subsurface.

Previous studies have examined the role of oxygen vacancies in the context of metal-oxide gas sensors based on ex situ characterization or simulation, see e.g. Refs. 4, 8-10. Sintered semiconductor grains are non-stoichiometric and, as such, contain oxygen vacancies distributed over the grain.[10] In addition, as described above, the dynamic formation of oxygen vacancies upon exposure to target gases has been proposed (see e.g. Refs. 4, 11 and references therein), but has not been reported for working gas sensors so far. Summarizing, to enhance the knowledge-based design of better gas sensors, new experimental approaches need to be developed that enable the assessment of gas-sensing mechanisms directly under working conditions of the gas sensor, i.e., by using *operando* approaches.

In this study, we demonstrate the potential of combined *operando* Raman–gas-phase Fourier transform infrared (FTIR) spectroscopy to elucidate the mode of operation of ceria doped with 0.5 wt% gold (Au/CeO_2) during ethanol gas sensing. In particular, Raman spectroscopy makes it possible to directly monitor the presence of oxygen vacancies in ceria besides surface species, while simultaneously recorded FTIR spectra capture the gas-phase composition. As a result, such *operando* studies allow us to explore the relation of the spectroscopic (structural) information to the resistance changes under the working conditions of the gas sensor. While mass spectrometry has been a more common technique in gas-phase analysis, the use of IR spectroscopy allows a direct coupling to the outlet of the *operando* cell, as well as a

straightforward signal assignment due to its chemical specifity, and may therefore be of broader interest for similar studies.

The left of Figure 1 depicts a typical low-wavenumber Raman spectrum of the Au/CeO_2 gas sensor at 400°C in air, which is dominated by the intense F_{2g} mode of ceria.[12,13] For details of the preparation and characterization of the Au/CeO_2 gas sensor please refer to the Supporting Information. The right panel of Figure 1 illustrates the dependence of the F_{2g} position on temperature and gas environment. To ensure the removal of adsorbates, the gas sensor was calcined at 400°C in air after each temperature treatment. As a result of lattice expansion, with increasing temperature a redshift of the F_{2g} band is observed. For constant temperature, switching from nitrogen to 250 ppm EtOH in nitrogen ($EtOH/N_2$) leads to a downshift of the F_{2g} band, indicating a relation between the gas environment and the ceria (defect) structure. In fact, in previous theoretical studies based on DFT+U (density functional theory + U), a relation between changes δ in the ceria stoichiometry $CeO_{2-\delta-x}$ due to increasing oxygen-vacancy concentration and the redshift of the F_{2g} band position ($\Delta\omega$) of $\delta = 0.024 \pm 0.005\ \Delta\omega/cm^{-1}$ has been found,[13,14] i.e., a redshift of 1 cm^{-1} corresponds to a change in stoichiometry of δ = 0.024. Therefore, the position of the F_{2g} mode can serve as a sensitive (quantitative) indicator of changes in the oxygen vacancy concentration in the subsurface upon exposure to ethanol. The temperature-dependent changes in oxygen vacancy concentration upon EtOH exposure suggest an increase in the ethanol reaction rate that is higher than the refilling of the vacancies by oxygen diffusion (see discussion below).

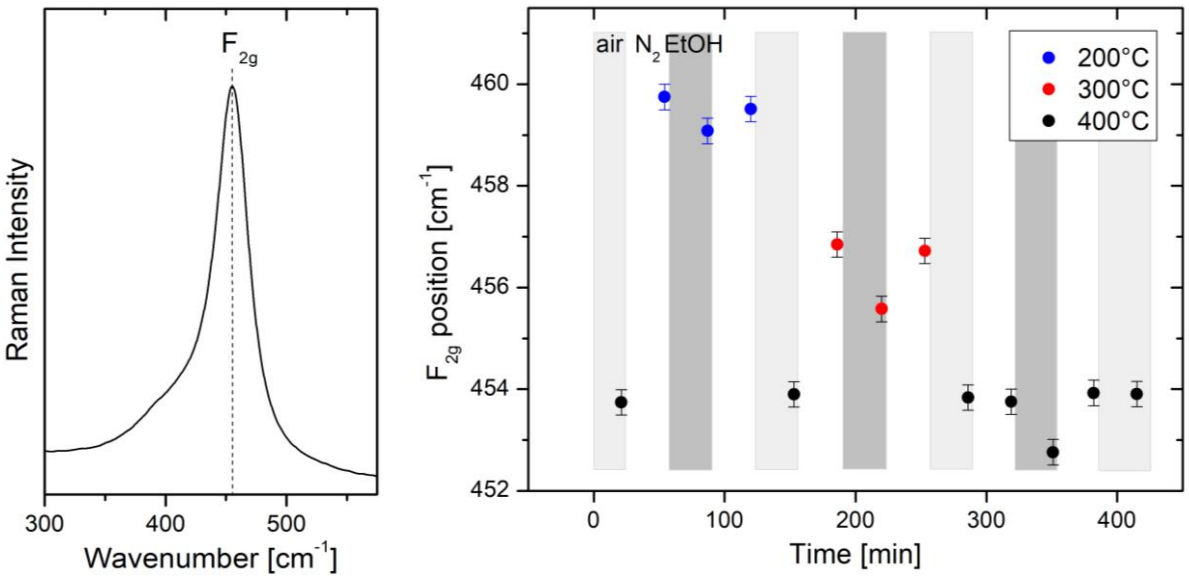

Figure 1. Left: Raman spectrum of the Au/CeO_2 gas sensor at 400°C in air at 514.5 nm excitation showing the spectral region around the F_{2g} band. **Right:** F_{2g} band position of the Au/CeO_2 gas sensor as a function of temperature and gas composition. Light gray areas correspond to O_2/N_2 (air), dark gray areas to 250 ppm $EtOH/N_2$, and white areas to N_2 exposure. See text for details.

Figure 2 depicts results of the simultaneous measurement of the sensor resistance, the position of the Raman F_{2g} band, and FTIR spectra of the gas-phase products (see Figure S-3 for a scheme of the experimental setup and Figure S-4 for Raman spectra). As will be discussed in detail in the following, this data set can be used to reveal correlations of the sensor resistance and the spectroscopic features. The assignment of the IR gas-phase bands is summarized in Table 1.

Table 1. Assignment of the IR gas-phase bands used for the correlation in Figure 2.

wavenumber (cm^{-1})	gas
2903	EtOH
2361	CO_2
2733	H_3C-CH=O

As shown in Figure 2, switching from 400°C (air) to 190°C (N_2) leads to an increase in the resistance, in accordance with the temperature dependence of a normal semiconductor. Upon switching the gas atmosphere from nitrogen to 250 ppm EtOH/N_2 at 190°C, a resistance decrease is observed owing to a release of electrons into the conduction band, as expected for an n-type semiconductor gas sensor exposed to a reducing gas. As reaction products, mainly carbon dioxide, acetaldehyde, and water (not shown) were detected, whereas the concentration of ethylene is at the FTIR detection limit (not shown). For other metal-oxide gas sensors the formation of acetaldehyde has been proposed to proceed via adsorbed ethoxy undergoing dehydrogenation, [15,16] while CO_2 is known to be formed as result of alcohol oxidation over ceria-supported gold systems, e.g. resulting from consecutive oxidation of alkoxy species and formates.[17] During exposure of the gas sensor to EtOH/N_2, the F_{2g} band shows a 0.5 cm^{-1} redshift as a result of oxygen-vacancy formation, corresponding to a change δ in the ceria stoichiometry $CeO_{2-\delta-x}$ of 0.012. Note that the value of the F_{2g} position represents an average value obtained on the basis of the Raman spectrum recorded during the duration of EtOH/N_2 exposure (~20 min). Switching back to pure nitrogen induces only a small increase in resistance. A similar effect has been observed previously for ethanol gas sensing on In_2O_3 and has been attributed to the presence of stable acetate adsorbates formed during EtOH/N_2 exposure, which prevent the sensor from returning to its initial state.[6,16] In fact, although no adsorbed species are visible in the Raman spectra under these conditions, the IR signal shows that there is still CO_2 desorption from the sensor surface, indicating the presence of adsorbates, in concentrations below the Raman detection limit for Au/CeO_2, undergoing surface reactions. It should be mentioned that for a bare ceria gas sensor we were able to show the presence of adsorbed acetate, formate, and ethanol species under these conditions (see Figure S-5 and accompanying detailed data description), showing a behavior similar to that observed previously for indium

oxide gas sensors.[6,16] Interestingly, in pure nitrogen the F_{2g} band shows a blueshift back to its position prior to EtOH/N_2 exposure. This can be rationalized by the filling of oxygen vacancies by oxygen diffusing from the bulk to the subsurface region, which is sampled by the Raman experiment (see Supporting Information for details on the Raman probe depth).[18]

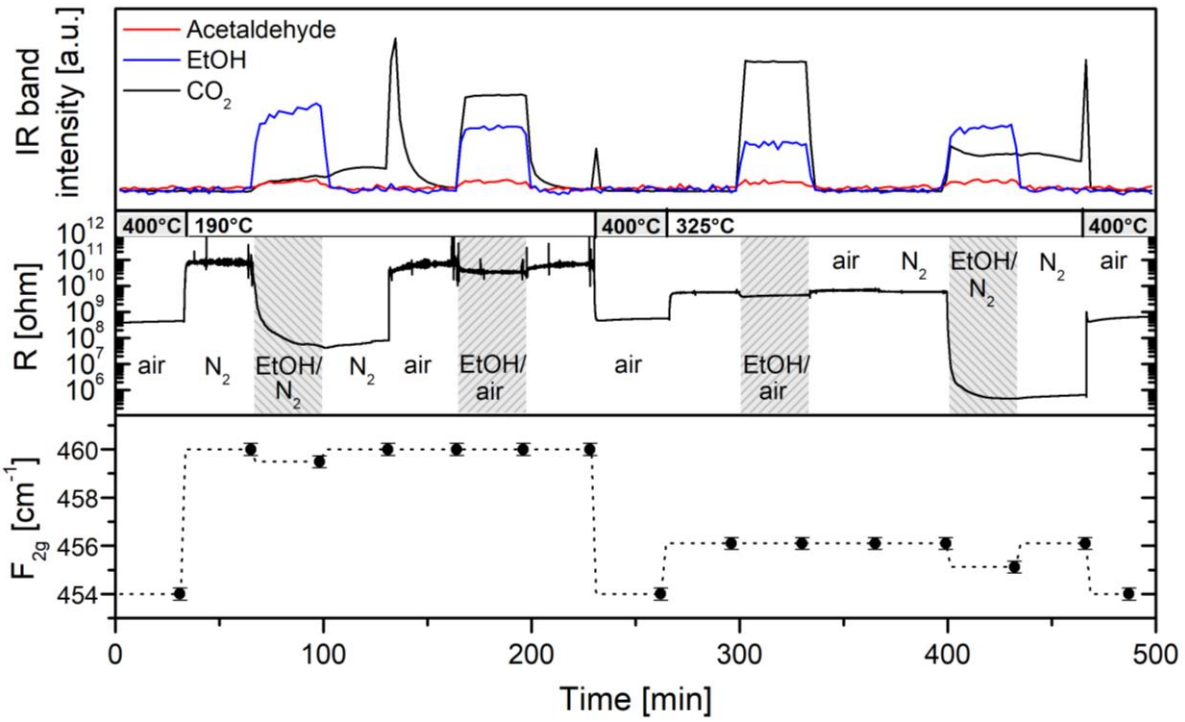

Figure 2. Temporal correlation of spectroscopic data and sensor resistance of the *operando* Raman–FTIR experiment during ethanol gas sensing of Au/CeO_2. F_{2g} band positions are based on Raman spectra recorded at 514.5 nm excitation. The dashed line is a guide to the eye.

When oxygen is added, the CO_2 signal shows an immediate increase, indicating the decomposition and further oxidation of adsorbates. As a result, a prompt increase of the sensor resistance is observed, which can be explained by the fast reoxidation of the sensor surface, removing electrons from the conduction band. Upon exposure to 250 ppm ethanol in air, a decrease in resistance is observed. However, the resistance decrease is less pronounced than in EtOH/N_2 owing to permanent reoxidation of the gas sensor by oxygen, resulting in an overall

smaller degree of reduction. In contrast to the behavior in EtOH/N_2, under these more oxidizing conditions, no oxygen-vacancy formation is detected. As reaction products acetaldehyde, carbon dioxide, and water were observed. The main product, carbon dioxide, was formed at a higher rate than in the reaction in EtOH/N_2, resulting in a larger conversion of ethanol. Switching back to air leads to an immediate increase in resistance followed by a slower continuous increase to the value before EtOH/air exposure. The slow resistance increase may be attributed to the decrease in adsorbate concentration, as indicated by the CO_2 signal.

Before the next set of experiments, at 325°C, the sensor was heated to 400°C to remove all adsorbates from the surface. Decomposition and/or desorption of the remaining adsorbates by thermal decomposition results in the formation of CO_2 and H_2O as identified by FTIR spectroscopy. As expected for normal semiconductor behavior, the resistance shows a decrease when heated to 400°C in air, returning to its initial value at the first stage of the experiment. When the temperature was decreased to 325°C, the resistance increased, again in agreement with normal semiconductor behavior. The temperature-dependent behavior of the F_{2g} band position upon heating to 400°C (i.e., F_{2g} redshift) and subsequent cooling to 325°C (i.e., F_{2g} blueshift) is in full accordance with the behavior depicted in Figure 1.

Upon switching to 250 ppm ethanol in air at 325°C, a significantly higher gas product concentration of CO_2 was observed than at 190°C, while acetaldehyde showed a similar concentration. The resistance showed a small decrease, which immediately increased to its value before EtOH exposure, when the feed was switched back to air. Under these conditions, no adsorbates are detected based on FTIR spectroscopy, consistent with the faster product formation at 325°C. Switching from air to nitrogen resulted in a minor decrease of the resistance, which may be explained by an (spectroscopically undetectable) increase in the concentration of oxygen vacancies.

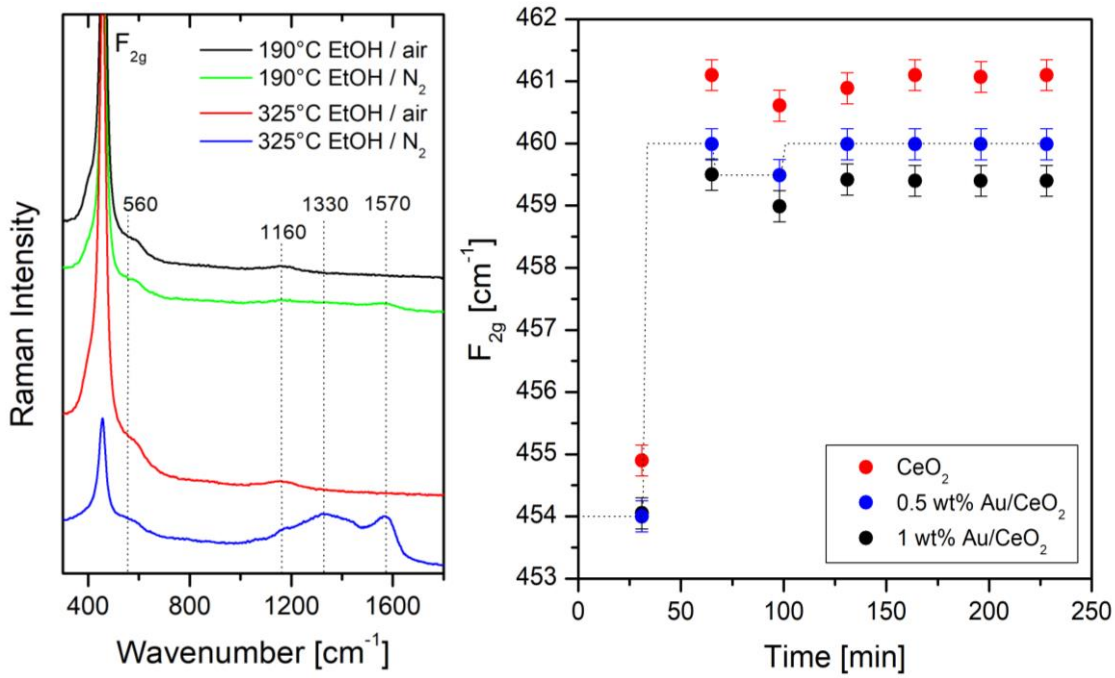

Figure 3. Left: *Operando* Raman spectra of the ethanol gas sensing by Au/CeO_2 recorded at 514.5 nm excitation. The F_{2g} band is cut off, the F_{2g} band positions correspond to those given in Figure 2. Spectra are offset for clarity. **Right:** Comparison of F_{2g} band positions for CeO_2, 0.5 wt% Au/CeO_2, and 1 wt% Au/CeO_2 gas sensors during ethanol gas sensing. The dashed line is a guide to the eye.

Exposure to 250 ppm EtOH in nitrogen at 325°C leads to a decrease in the resistance, which is significantly stronger than in EtOH/air owing to the absence of reoxidation of the sensor by oxygen. In comparison to 190°C a higher ethanol conversion was observed. As discussed above, mainly the total oxidation product CO_2 is detected. The left panel of Figure 3 shows, that new Raman bands appear at around 1330 cm^{-1} and 1570 cm^{-1}, which have been assigned to the D and G bands of carbon, respectively, indicating the decomposition of ethanol on the sensor surface, while the ceria-related bands at around 560 cm^{-1} (Ce^{3+}-related bulk defects [13,14]) and at 1160 cm^{-1} (2LO [12,13]) show no significant changes in intensity (see Supporting Information).

During exposure to EtOH/N_2, a mode-softening of the F_{2g} band by 1 cm^{-1} is observed, caused by oxygen-vacancy formation, corresponding to a change δ in the ceria stoichiometry of 0.024 (see above). The higher concentration of oxygen vacancies as compared to 190°C can be rationalized by the increased reactivity of ethanol at 325°C overwhelming the faster oxygen diffusion. When the feed was switched back to pure nitrogen, only a small increase in resistance was observed. As discussed before in the context of the 190°C data, this behavior is attributed to the presence of adsorbates formed during EtOH/N_2 exposure – inter alia carbon species (see Figure 3) – preventing the sensor from returning to its initial state.[6,16] This is also supported by the continuous CO_2 desorption from the sensor surface detected by FTIR spectroscopy. Upon switching to pure nitrogen, the F_{2g} band shifts back to its position prior to EtOH/N_2 exposure, resembling the behavior at 190°C. As discussed above, the observed blueshift is attributed to the filling of oxygen vacancies by oxygen diffusion to the subsurface region sampled by Raman spectroscopy (see above). Finally, the sensor is heated to 400°C in air, resulting in an immediate increase in resistance caused by fast reoxidation of the surface, leading to removal of electrons from the conduction band. This is accompanied by the decomposition and further oxidation of adsorbates, resulting in a strong but narrow CO_2 signal. The smaller CO_2 area than at 190°C (after 130 min) can be rationalized by the higher conversion and therefore smaller amount of adsorbates present at the surface at higher sensor temperature.

The mode-softening of the F_{2g} band due to oxygen-vacancy formation was also observed for other CeO_2-based gas sensors. The right of Figure 3 shows a comparison of F_{2g} band positions for CeO_2, 0.5 wt% Au/CeO_2, and 1 wt% Au/CeO_2 during ethanol gas sensing. The experimental conditions correspond to those discussed above for 0.5 wt% Au/CeO_2 (see Figure 2 and Supporting Information). In comparison to bare ceria, for Au-loaded samples a stronger redshift in the initial F_{2g} band position, corresponding to a higher oxygen-vacancy concentration, is observed. This behavior is in agreement with the prediction from theory and previous

experimental studies.[14,19] Importantly, despite their different initial states, all gas sensors show a comparable F_{2g} mode-softening upon exposure to 250 ppm EtOH in nitrogen, highlighting the importance of the metal-oxide semiconductor material for oxygen- vacancy formation.

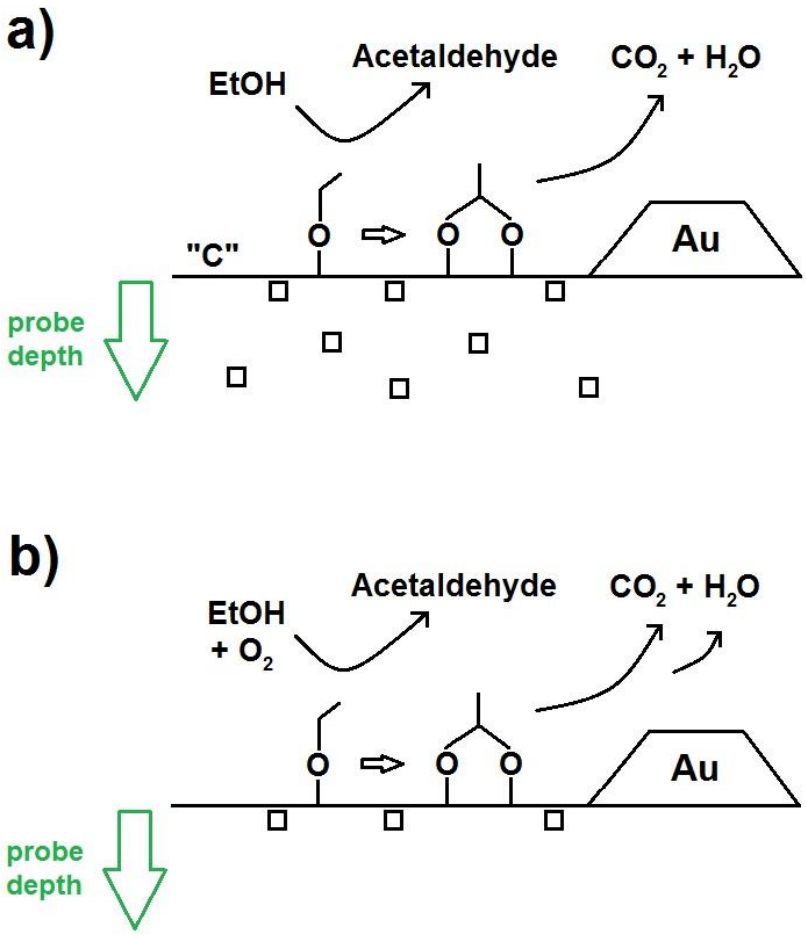

Figure 4. Proposed mechanism for the sensing of ethanol gas by Au/CeO_2 (a) without and (b) with oxygen being present. "C" represents adsorbed carbon species. The symbol □ represents an oxygen vacancy. The probe depth indicates the Raman sampling depth during the *operando* experiments. For details see text.

The above findings demonstrate the potential of the combined *operando* Raman–gas phase FTIR spectroscopic approach for providing new fundamental insight into the functioning of metal-oxide gas sensors. As a new piece of information, the use of Raman spectroscopy is shown to enable the direct and quantitative monitoring of the oxygen-vacancy dynamics in subsurface ceria via F_{2g} mode-softening under reducing conditions (see Figure 4a). In contrast, in the presence of gas-phase oxygen, no oxygen vacancies are observed, which we attribute to their reoxidation and/or confinement to the surface (see Figure 4b). Thus, on the basis of our combined spectroscopic results, we propose a mechanism for ethanol gas sensing by Au/CeO_2 as illustrated in Figure 4: In the $EtOH/N_2$ gas environment, the gas sensor is in its most strongly reduced state, forming acetaldehyde and the main products CO_2/H_2O most probably via ethoxide, formate, and acetate intermediates, respectively (see Figure 4a). Upon removal of EtOH, reoxidation of the sensor (subsurface) sets in, as confirmed by the observed F_{2g} blueshift (see Figures 2 and 3). The fact that the corresponding resistance changes do not correlate with the observed changes in oxygen vacancy concentration in the ceria subsurface strongly suggests a significant contribution of surface-related species such as surface oxygen and/or adsorbates to the sensor's response. As surface oxygen relevant to gas sensing, 'ionosorbed' oxygen species such as O^-, O_2^-, and O_2^{2-} have been discussed.[20] In this context it should be mentioned that the presence of ceria lattice oxygen has previously been shown to be accessible by the Ce-O longitudinal and transversal stretching modes of the topmost Ce-O layer at around 250 and 400 cm^{-1}.[13,18] In $EtOH/N_2$ flow, these features show a decrease in intensity, however, quantification is difficult due to the low-wavenumber cut-off and the overlap with the strong F_{2g} band (see Figure S-4). Also, please note that adsorbed superoxide or peroxide species were not observed under any of the gas-sensing conditions applied in this study, despite their recent Raman-spectroscopic detection on bare ceria in the presence of oxygen atmosphere (superoxide/peroxide) and on 0.5 wt% Au/CeO_2 (peroxide) in the context of the catalytic CO oxidation.[21,14] Thus, while there is recent progress in the detection of lattice and molecularly

adsorbed oxygen, it remains a tremendous challenge to access the relevant surface-oxygen species under working conditions of metal-oxide based gas sensors in a quantitative manner.

Interestingly, the observed behavior is in contrast to that of the same Au/CeO_2 material during catalytic CO oxidation, where a direct correlation between catalytic activity and oxygen vacancy concentration was observed.[14] We attribute these findings to the very different partial pressures of reductant present under working conditions affecting the metal-oxide defect structure to a different extent. Thus, by using *operando* spectroscopy, important differences between the mode of operation of gas sensors and catalysts can be deduced.

Supporting Information

Materials and methods, structural characterization; supporting Figures and Table.

Acknowledgements

This work was supported by the Deutsche Forschungsgemeinschaft (DFG). The authors thank Silvio Heinschke for performing nitrogen adsorption/desorption experiments, and Karl Kopp for X-ray photoelectron spectroscopy (XPS) analysis and technical support.

References

1 Williams, D. E. Semiconducting Oxides as Gas-Sensitive Resistors. *Sens. Actuators, B* **1999**, *57*, 1-16.

2 Barsan, N.; Koziej, D.; Weimar, U. Metal Oxide-Based Gas Sensor Research: How to? *Sens. Actuators B* **2007***, 121*, 18-35**.**

3 Korotcenkov, G. Metal Oxides for Solid-State Gas Sensors: What Determines Our Choice? *Mater. Sci. Eng. B* **2007***, 139*, 1-23.

4 Gurlo, A.; Riedel, R. In Situ and Operando Spectroscopy for Assessing Mechanisms of Gas Sensing. *Angew. Chem. Int. Ed.* **2007**, *46*, 3826-3848.

5 Dey, A. Semiconductor Metal Oxide Gas Sensors: A Review. *Mater. Sci. Eng. B* **2018**, *229*, 206-217.

6 Sänze, S.; Gurlo, A.; Hess, C. Monitoring Gas Sensors at Work: Operando Raman-FTIR Study of Ethanol Detection by Indium Oxide. *Angew. Chem. Int. Ed.* **2013***, 52***,** 3607-3610.

7 Degler, D.; Rank, S.; Müller, S.; Pereira de Carvalho, H. W.; Grunwaldt, J.-D.; Weimar, U.; Barsan, N. Gold-Loaded Tin Dioxide Gas Sensing Materials: Mechanistic Insights and the Role of Gold Dispersion, *ACS Sens.* **2016**, *1*, 1322-1329.

8 Zhang, L.; Fang, Q.; Huang, Y.; Xu, K.; Chu, P. K.; Ma, F. Oxygen Vacancy Enhanced Gas-Sensing Performance of CeO_2/Graphene Heterostructure at Room Temperature. *Anal. Chem.* **2018**, *90*, 9821-9829.

9 Wang, D.; Sun, J.; Cao, X.; Zhu, Y.; Wang, Q.; Wang, G.; Han, Y.; Lu, G.; Pang, G.; Feng, S. High-Performance Gas Sensing Achieved by Mesoporous Tungsten Oxide Mesocrystals with Increased Oxygen Vacancies. *J. Mater. Chem. A* **2013**, *1*, 8653-8657.

10 Liu, J.; Gao, Y.; Wu, X.; Jin, G.; Zhai, Z.; Liu, H. Inhomogeneous Oxygen Vacancy Distribution in Semiconductor Gas Sensors: Formation, Migration and Determination on Gas Sensing Characteristics. *Sensors* **2017**, *17*, 1852, doi:10.3390/s17081852.

11 Kolmakov, A.; Moskovits, M. Chemical Sensing and Catalysis by One-Dimensional Metal-Oxide Nanostructures. *Annu. Rev. Mater. Res.* **2004**, *34*, 151-180.

12 Filtschew, A.; Hofmann, K.; Hess, C. Ceria and Its Defect Structure: New Insights from a Combined Spectroscopic Approach. *J. Phys. Chem. C* **2016**, *120*, 6694-6703.

13 Schilling, C.; Hess, C.; Ganduglia-Pirovano, M. V. Raman Spectra of Polycrystalline CeO_2: A Density Functional Theory Study. *J. Phys. Chem. C* **2017**, *121*, 20834-20849.

14 Schilling, C.; Hess, C. Real-Time Observation of the Defect Dynamics in Working Au/CeO_2 Catalysts by Combined Operando Raman/UV-Vis Spectroscopy. *J. Phys. Chem. C* **2018**, *122*, 2909-2917.

15 Kohl, D. *Sens. Actuators* **1989**, *18*, 71–113.

16 Sänze, S.; Hess, C. Ethanol Gas Sensing by Indium Oxide: An Operando Spectroscopic Raman-FTIR Study. *J. Phys. Chem. C* **2014**, *118*, 25603-25613.

17 Rousseau, S.; Marie, O.; Bazin, P.; Daturi, M.; Verdier, S.; Harlé, V. Investigation of Methanol Oxidation over Au/Catalysts Using Operando IR Spectroscopy: Determination of the Active Sites, Intermediate/Spectator Species, and Reaction Mechanism. *J. Am. Chem. Soc.* **2010**, *132*, 10832–10841.

18 Schilling, C.; Hess, C. Elucidating the Role of Support Oxygen in the Water–Gas Shift Reaction over Ceria-Supported Gold Catalysts Using Operando Spectroscopy. *ACS Catal.* **2019**, *9*, 1159–1171.

19 Lee, Y.; He, G.; Akey, A. J.; Si, R.; Flytzani-Stephanopoulos, M.; Herman, I. P. Raman Analysis of Mode Softening in Nanoparticle $CeO_{2-\delta}$ and Au-$CeO_{2-\delta}$ during CO Oxidation. *J. Am. Chem. Soc.* **2011**, *133*, 12952−12955.

20 Gurlo, A. Interplay Between O_2 and SnO_2: Oxygen Ionosorption and Spectroscopic Evidence for Adsorbed Oxygen. *ChemPhysChem* **2006**, *7*, 2041-2052.

21 Schilling, C.; Ganduglia-Pirovano, M. V.; Hess, C. Experimental and Theoretical Study on the Nature of Adsorbed Oxygen Species on Shaped Ceria Nanoparticles. *J. Phys. Chem. Lett.* **2018**, *9*, 6593-6598.

TOC graphic

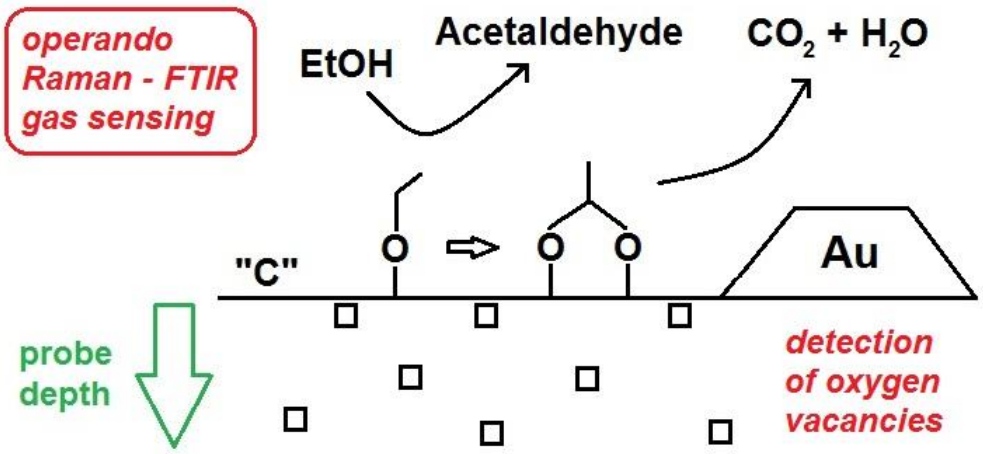
operando
Raman - FTIR
gas sensing
EtOH
Acetaldehyde
$CO_2 + H_2O$
"C"
O
O
O
Au
probe
depth
detection
of oxygen
vacancies